

Macrocyclic Heterodinuclear $Co^{II}M^{II}$ (M = Ni, Zn) Complexes. Ferromagnetic Interaction and EPR of $Co^{II}Ni^{II}$ ($S_{Co} = 1/2$, $S_{Ni} = 1$) Complex

Kazutoshi Danjobara, Yuko Mitsuka, Yuji Miyasato, Masaaki Ohba, and Hisashi Ōkawa*

Department of Chemistry, Faculty of Science, Kyushu University, Hakozaki, Higashiku 6-10-1, Fukuoka 812-8581

Received March 31, 2003; E-mail: okawascc@mbox.nc.kyushu-u.ac.jp

The dinucleating compartmental ligand $(L^{2,3})^{2-}$, derived from the [2:1:1] cyclic condensation of 2,6-diformyl-4-methylphenol, ethylenediamine and 1,3-trimethylenediamine, has formed heterodinuclear $Co^{II}M^{II}$ complexes, $[CoM(L^{2,3})](ClO_4)_2 \cdot H_2O \cdot 0.5CH_3CN$ (M = Ni (**1**), Zn (**2**)). Crystallographic studies for $[CoNi(L^{2,3})(CH_3CN)_3](ClO_4)_2 \cdot 2MeOH \cdot 0.5H_2O$ (**1′**) indicate that the Co^{II} is bound to the N_2O_2 site formed with ethylenediamine and has a square-pyramidal geometry with one acetonitrile molecule at the apex. The Ni is bound to the N_2O_2 site formed with 1,3-trimethylenediamine and has a pseudo octahedral geometry with two acetonitrile molecules at the axial sites. Complex **1** shows a ferromagnetic interaction between the Co^{II} ($S = 1/2$) and Ni^{II} ($S = 1$) ions and a frozen DMF solution of **1** at liquid nitrogen temperature exhibits EPR signals attributable to the $S_T = 3/2$ ground state with a zero-field splitting of $D = 0.095$ cm^{-1}. The cryomagnetic property is simulated, based on isotropic model ($H = -2JS_1S_2$) and by taking into consideration the zero-field splitting, to give an exchange integral of $J = +22$ cm^{-1}.

Study of magnetic interaction in heteronuclear metal complexes is important to understand the spin-exchange mechanism with respect to the ground-state electronic configurations of the constituting metal ions.[1] Magnetic properties of di(μ-phenolato)$Cu^{II}M^{II}$ complexes were extensively studied.[2–7] These works have clarified that an antiferromagnetic interaction occurs between Cu^{II} and M^{II} ions when the M^{II} has unpaired electron on its $d_{x^2-y^2}$ orbital, whereas a ferromagnetic interaction occurs when the M^{II} has unpaired electron(s) on its d orbital(s) other than $d_{x^2-y^2}$ orbital[3,4,8] (x and y axes are taken along donor atoms on the equatorial plane). A ferromagnetic interaction recognized for Cu^{II}–V^{IV}(=O) complexes is explained by the strict orthogonality of the magnetic orbitals, $d_{x^2-y^2}(Cu) \perp d_{xy}(V)$.[1,4]

Low-spin Co^{II} has one unpaired electron on either d_{z^2} orbital or $d_{xz}(d_{yz})$ orbital.[9] It is of interest to examine the magnetic interaction in heterodinuclear complexes with low-spin Co^{II} in view of its electronic structure, but magnetic studies for CoM complexes are very limited.[8] In this work the phenol-based dinucleating compartmental ligand $(L^{2,3})^{2-}$ (Fig. 1) is used to afford $[CoM(L^{2,3})](ClO_4)_2 \cdot H_2O \cdot 0.5CH_3CN$ (M = Ni (**1**), Zn (**2**)) (hereafter 'M_aM_b' complex or $[M_aM_b(L^{2,3})]^{n+}$ means that the M_a is bound to the site with the ethylene lateral chain and M_b is bound to the site with the trimethylene lateral chain). The CoNi complex is comprised of a low-spin Co^{II} ($S = 1/2$) and a high-spin Ni^{II} ($S = 1$) and shows a ferromagnetic interaction between the pair of metal ions to afford the $S_T = 3/2$ ground state. X-band EPR spectroscopic studies for the CoNi complex indicate a zero-field splitting of the ground spin state. Magnetic analysis for the complex has been carried out based on an isotropic model and by taking into consideration the zero-field splitting.

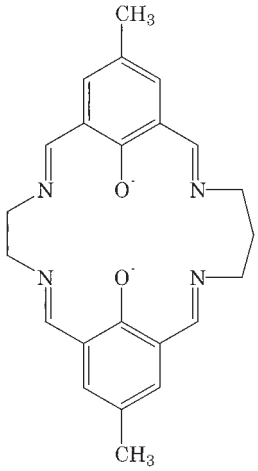

Fig. 1. The chemical structure of $(L^{2,3})^{2-}$.

Experimental

Physical Measurements. Elemental analyses of carbon, hydrogen and nitrogen were obtained at The Service Center of Elemental Analysis of Kyushu University. Metal analyses were obtained using a Shimadzu AA-680 Atomic Absorption/Flame Emission Spectrophotometer. Infrared spectra were measured using a KBr disk on a PERKIN ELMER Spectrum BX FT-IR system. FAB mass spectrometric measurements were carried out on a JMS-SX/SX102A Tandem mass spectrometer using *m*-nitrobenzylalcohol as the matrix. Electronic absorption spectra were recorded on a Shimadzu UV-3100PC Spectrophotometer. X-band EPR spectra were recorded using a JEOL JEX-FE3X spectrometer in frozen DMF solution at liquid nitrogen tem-

Published on the web September 15, 2003; DOI 10.1246/bcsj.76.1769

perature. Magnetic susceptibilities of powdered samples were measured on a Quantum Design MPMS XL SQUID susceptometer in the temperature range of 2–300 K. Diamagnetic corrections were made using Pascal's constants.[10]

Preparation. 2,6-Diformyl-4-methylphenol was prepared by the literature method.[11] $[Pb\{Co(L^{2,3})\}_2](ClO_4)_2\cdot 2CH_3OH$ was prepared by a method described in our previous paper.[6e] Other chemicals were purchased from commercial sources and used without further purification.

$[CoNi(L^{2,3})](ClO_4)_2\cdot H_2O\cdot 0.5CH_3CN$ (1). A solution of $Ni(ClO_4)_2\cdot 6H_2O$ (137 mg, 0.375 mmol) in methanol (10 cm^3) and a suspension of $[Pb\{Co(L^{2,3})\}_2](ClO_4)_2\cdot 2CH_3OH$ (1.024 g, 0.75 mmol) in methanol (10 cm^3) were mixed and stirred for 30 min. To this mixture was added a solution of $NiSO_4\cdot 6H_2O$ (99 mg, 0.375 mmol) in methanol (10 cm^3), and the resulting reddish solution was evaporated to dryness. The residue was triturated with acetonitrile (20 cm^3), insoluble $PbSO_4$ was separated by filtration, and the filtrate was diffused with ether to afford reddish brown plates. The yield was 640 mg (47%). Found: C, 39.16; H, 3.79; N, 8.37; Co, 7.42; Ni, 7.52%. Calcd for $C_{24}H_{27.5}N_{4.5}Cl_2CoNiO_{11}$: C, 38.76; H, 3.73; N, 8.48; Co, 7.93; Ni, 7.89%. μ_{eff} per CoNi: 3.71 μ_B at 298 K. Selected IR (ν/cm^{-1}) on KBr: 3437, 2925, 2360, 1630, 1555, 1456, 1330, 1109, 1090, 1043, 819, 766, 625, 520. Vis [λ/nm (ε/$M^{-1}\,cm^{-1}$)] in DMF: 570 (1000^{sh}), 1250 (8), 1450 (10).

$[CoZn(L^{2,3})](ClO_4)_2\cdot H_2O\cdot 0.5CH_3CN$ (2). This was obtained as red plates in a way similar to that for **1** using $Zn(ClO_4)_2\cdot 6H_2O$ and $ZnSO_4\cdot 7H_2O$. The yield was 44%. Found: C, 38.43; H, 3.59; N, 8.22; Co, 7.53; Zn, 8.74%. Calcd for $C_{24}H_{27.5}N_{4.5}Cl_2CoO_{11}Zn$: C, 38.42; H, 3.69; N, 8.40; Co, 7.86; Zn, 8.72%. μ_{eff} per CoZn: 1.87 μ_B at 298 K. Selected IR (ν/cm^{-1}) on KBr: 3430, 2926, 2362, 1633, 1557, 1451, 1323, 1114, 1092, 1045, 816, 767, 624, 510. Vis [λ/nm (ε/$M^{-1}\,cm^{-1}$)] in DMF: 570 ($\sim 750^{sh}$), 1450 (13).

Structure Analysis. Efflorescent single crystals of $[CoNi(L^{2,3})(CH_3CN)_3](ClO_4)_2\cdot 2MeOH\cdot 0.5H_2O$ (**1′**) were obtained by the recrystallization of **1** from an acetonitrile–methanol mixture. Crystallographic measurements were carried out at -90 ± 1 °C on a Rigaku/MCS Mercury diffractometer, using graphite monochromated Mo-Kα radiation ($\lambda = 0.71069$ Å) and a 12 kW rotating anode generator. Crystallographic parameters are summarized in Table 1.

The structure was solved by the direct method and expanded using Fourier techniques. The non-hydrogen atoms were refined anisotropically. Hydrogen atoms were included in the structure factor calculation but not refined. Computations were carried out on a SGI O2 computer using TeXsan crystallographic software package.[12]

Crystallographic data have been deposited at the CCDC, 12 Union Road, Cambridge CB2 1EZ, UK and copies can be obtained on request, free of charge, by quoting the publication citation and deposition numbers CCDC 210803.

Table 1. Crystallographic Parameters for $[CoNi(L^{2,3})(CH_3CN)_3](ClO_4)_2\cdot 2MeOH\cdot 0.5H_2O$ (**1′**)

Complex	**1′**
Formula	$C_{31}H_{41}N_7Cl_2CoNiO_{10.5}$
F.w.	868.24
Crystal color	brown
Crystal size/mm^3	$0.37 \times 0.25 \times 0.20$
Crystal system	triclinic
Space group	$P\bar{1}$ (#2)
a/Å	11.8425(1)
b/Å	12.4617(1)
c/Å	15.8858(7)
α/°	75.941(17)
β/°	79.981(18)
γ/°	64.806(13)
V/$Å^3$	2051.167(1)
Z	2
D_{calcd}/g cm^{-3}	1.406
μ(Mo-Kα)/cm^{-1}	10.53
No. of reflections	3892
	($I > 3.00\sigma(I)$)
R	0.081
R_w	0.120

Results and Discussion

Preparation and General Properties. The $Cu^{II}M^{II}$ and $Ni^{II}M^{II}$ complexes of $(L^{2,3})^{2-}$ and analogous macrocyclic ligands have been obtained by the stepwise template reaction developed in our laboratory.[6,13] This method was applied to the preparation of the $Co^{II}M^{II}$ complexes in this work. The Co_2Pb precursor complex $[Pb\{Co(L^{2,3})\}_2](ClO_4)_2\cdot 2CH_3OH$ was prepared by the cyclization of *N*,*N*′-ethylenedi(3-formyl-5-methylsalicylaldiminato)cobalt(II) with 1,3-trimethylenediamine in the presence of $Pb(ClO_4)_2$ and then converted into $Co^{II}M^{II}$ complexes (M = Ni(**1**), Zn(**2**)) by the transmetallation reaction using one-half molar amount each of metal(II) sulfate and metal(II) perchlorate.

The FAB mass spectrum of **1** has a group of ion peaks centered around $m/z = 604.0$ corresponding to $\{CoNi(L^{2,3})(ClO_4)\}^+$. Another group of ion peaks centered around $m/z = 505.1$ corresponds to $\{CoNi(L^{2,3})\}^+$. Similarly, the FAB mass spectrum of **2** has two dominant ion peaks centered around $m/z = 610.1$ and 511.1, which are ascribed to $\{CoZn(L^{2,3})(ClO_4)\}^+$ and $\{CoZn(L^{2,3})\}^+$, respectively. In our attempts to prepare other $Co^{II}M^{II}$ (M = Mn, Fe, Cu) complexes of $(L^{2,3})^{2-}$, a scrambling of metal ions occurred to afford a mixture of homodinuclear and heterodinuclear complexes. An acetato$Co^{II}Mn^{II}$ complex of $(L^{2,3})^{2-}$, $[CoMn(L^{2,3})(AcO)(DMF)]ClO_4$, has been derived from the Co_2Pb precursor complex by a similar transmetallation reaction in the presence of sodium acetate.[6e] In this complex, the acetate group bridges the two metal ions and contributes to the stabilization of the $Co^{II}Mn^{II}$ heterodinuclear core.

It is important to see the magnetic nature of the Co in the CoZn complex (**2**) in order to investigate the magnetic interaction in the CoNi complex (**1**). Complex **2** has a magnetic moment of 2.07 μ_B at room temperature. Evidently it has a low-spin electronic structure. A frozen DMF solution of **2** shows an axial pattern of EPR of $g_\parallel = 2.01$ and $g_\perp = 2.24$ with a Co hyperfine structure ($A_{Co} = 100 \times 10^{-4}$ cm^{-1}) superimposed on the $g_\parallel$ component (Fig. 2). The EPR spectrum clearly indicates that the Co^{II} has one unpaired electron on its d_{z^2} orbital.[9] The magnetic property of **1** is discussed in detail later.

Both **1** and **2** are sensitive to dioxygen in solution, as can be inferred from the Co environment similar to Co(salen) (salen = *N*,*N*′-ethylenedi(salicylideneaminate)). The absorption

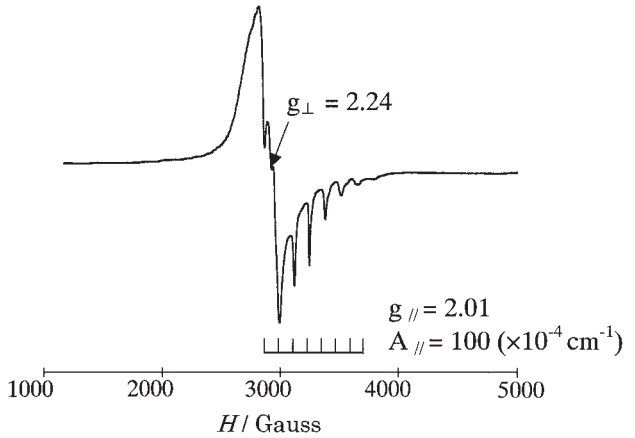

Fig. 2. EPR spectrum of **2** determined in a frozen DMF solution at liquid nitrogen temperature.

spectra of **1** and **2** in DMF show a weak near IR band at ~7000 cm^{-1} that is characteristic of Co(salen).[14–16] They show a moderately intense band at ~550 nm which is also characteristic of Co(salen) and related complexes.[15–17]

The ν_3 vibration mode of perchlorate group of **1** splits into three (1109, 1090 and 1043 cm^{-1}). This fact means that the perchlorate ion is involved in bidentate coordination.[18] It is likely that the Co^{II} and Ni^{II} ions have a five- or six-coordinate geometry together with perchlorate oxygen and water molecule. Such splitting of the ν_3 mode is also recognized for **2** (1114, 1092, 1045 cm^{-1}).

$[CoNi(L^{2,3})](ClO_4)_2 \cdot H_2O \cdot 0.5CH_3CN$ (**1**) prepared in this work and $[NiCo(L^{2,3})](ClO_4)_2 \cdot H_2O$ reported previously[6d] are regarded as coordination-position isomers when we ignore exogenous donating and solvating molecules. It must be mentioned that each of the CoNi and NiCo complexes are stabilized by macrocyclic effect[19] not to cause scrambling of metal ions or isomerization in solution.

Crystal Structure. X-ray structural studies have been made for $[CoNi(L^{2,3})(CH_3CN)_3](ClO_4)_2$ (**1′**). The crystallographic result is imperfect due to the poor quality of crystal used, but has clarified the dinuclear structure of **1′**. An ORTEP drawing of the structure is shown in Fig. 3. Selected bond distances and angles are given in Table 2.

In the crystal of **1′**, the Co resides in the cavity with the ethylene lateral chain and the Ni in the adjacent cavity with the trimethylene chain. The Co–Ni interatomic separation bridged by two phenolic oxygen atoms is about 3.0 Å. The Ni has a pseudo octahedral geometry together with two acetonitrile molecules at the axial sites. The in-plane Ni-to-donor bond distances range from 2.00 to 2.02 Å and the two axial Ni–N(acetonitrile) bond distances are 2.14 and 2.15 Å. The Co has a square-pyramidal geometry together with one acetonitrile molecule at the apex. The equatorial Co-to-donor bond distances fall in the range of 1.86–1.88 Å. The axial Co–N(acetonitrile) bond distance (2.17 Å) is significantly elongated. The short equatorial Co-to-donor bonds are in harmony with the low-spin state of the Co^{II} ion.[20]

Magnetic Property of CoNi Complex. The cryomagnetic property of **1** has been studied in the temperature range of 2–300 K and the μ_{eff} vs T plots is given in Fig. 4. The magnetic moment at room temperature is 3.71 μ_B per CoNi, and the moment increased slowly with decreasing temperature to reach a maximum moment of 3.97 μ_B at 20.0 K and then decreased below this temperature. Such magnetic behavior can be reasonably explained by the ferromagnetic interaction between Co^{II} ($S = 1/2$) and Ni^{II} ($S = 1$) centers affording the $S_T = 3/2$ ground state. The drop in magnetic moment at low temperature may arise from a secondary effect such as the zero-field splitting of the $S_T = 3/2$ ground state.

The ferromagnetic interaction in **1** is supported by EPR studies. The complex **1** is EPR-silent at room temperature

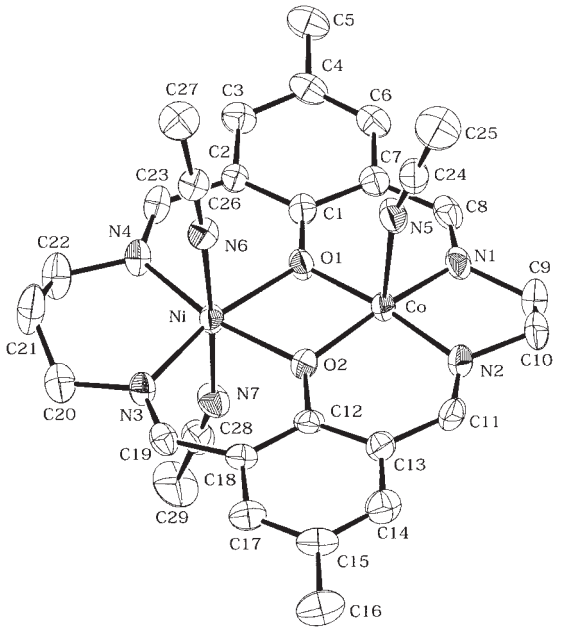

Fig. 3. A drawing of the structure of $[CoNi(L^{2,3})(CH_3CN)_3](ClO_4)_2 \cdot 2MeOH \cdot 0.5H_2O$ (**1′**).

Table 2. Selected Bond Lengths (Å) and Angles (°) for $[CoNi(L)(CH_3CN)_3](ClO_4)_2 \cdot 2MeOH \cdot 0.5H_2O$ (**1′**)

Distances			
Co–O(1)	1.886(7)	Ni–O(1)	2.013(6)
Co–O(2)	1.874(7)	Ni–O(2)	2.017(6)
Co–N(1)	1.866(9)	Ni–N(3)	2.002(8)
Co–N(2)	1.854(9)	Ni–N(4)	2.007(8)
Co–N(5)	2.16(1)	Ni–N(6)	2.130(9)
Co···Ni	3.002(2)	Ni–N(7)	2.149(9)
Angles			
Co–O(1)–Ni	100.6(3)	O(1)–Ni–N(4)	91.0(3)
Co–O(2)–Ni	100.9(3)	O(1)–Ni–N(6)	91.0(3)
O(1)–Co–O(2)	82.4(3)	O(1)–Ni–N(7)	89.6(3)
O(1)–Co–N(1)	94.0(3)	O(2)–Ni–N(3)	90.6(3)
O(1)–Co–N(2)	171.8(3)	O(2)–Ni–N(4)	166.7(3)
O(1)–Co–N(5)	97.1(3)	O(2)–Ni–N(6)	90.3(3)
O(2)–Co–N(1)	167.8(3)	O(2)–Ni–N(7)	94.2(3)
O(2)–Co–N(2)	94.3(4)	N(3)–Ni–N(4)	102.7(3)
O(2)–Co–N(5)	100.2(3)	N(3)–Ni–N(6)	91.4(3)
N(1)–Co–N(2)	87.7(4)	N(3)–Ni–N(7)	89.2(3)
N(1)–Co–N(5)	91.8(3)	N(4)–Ni–N(6)	88.4(3)
N(2)–Co–N(5)	90.9(4)	N(4)–Ni–N(7)	87.1(3)
O(1)–Ni–O(2)	75.9(3)	N(6)–Ni–N(7)	175.5(3)
O(1)–Ni–N(3)	166.2(3)		

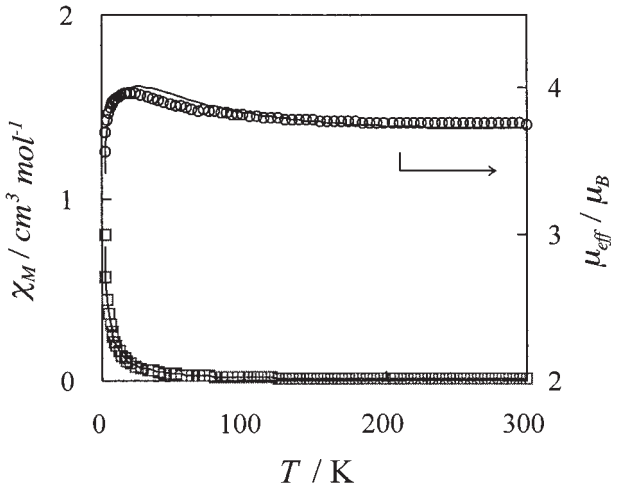

Fig. 4. Temperature-dependence of magnetic moment and magnetic susceptibility of **1**. The solid line is drawn based on the expression (1) using magnetic parameters of $J = +22.0$ cm^{-1}, $D = 0.095$ cm^{-1}, $g = 2.11$, $\theta = -0.50$ K and $N\alpha = 300 \times 10^{-6}$ cm^3 mol^{-1}.

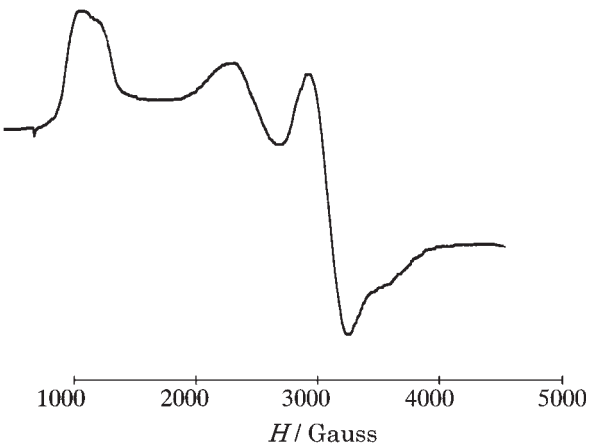

Fig. 5. EPR spectrum of **1** determined in a frozen DMF solution at liquid nitrogen temperature.

but shows three EPR signals at ~1050, ~2300 and ~3100 gauss when measured in a frozen DMF solution at liquid nitrogen temperature (Fig. 5). These signals must be associated with the $S_T = 3/2$ ground state. The energy diagram for $S_T = 3/2$ under an applied magnetic field parallel to the molecular axis (z) is given in Fig. 6 where the zero-field splitting parameter E is neglected.[21] The $S_T = 3/2$ state has a Kramers doublet ($M_S = \pm 1/2$) and the dominant EPR signal at ~3100 G ($g = 2.13$) can be assigned to the resonance between $M_S = +1/2$ and $-1/2$ under an applied field parallel to z axis. The presence of additional EPR resonance at lower magnetic field suggests that the zero-field splitting (2D) is small relative to the X-band microwave energy. One of the two low-field signals can be ascribed to the resonance between $M_S = +3/2$ and $+1/2$. If we suppose that the signal at ~1050 gauss corresponds to this resonance, the zero-field splitting parameter D is evaluated to be 0.095 cm^{-1} using $g = 2.13$. The remaining signal at ~2300 gauss can be a component of the transitions under an applied field perpendicular to the molecular axis.

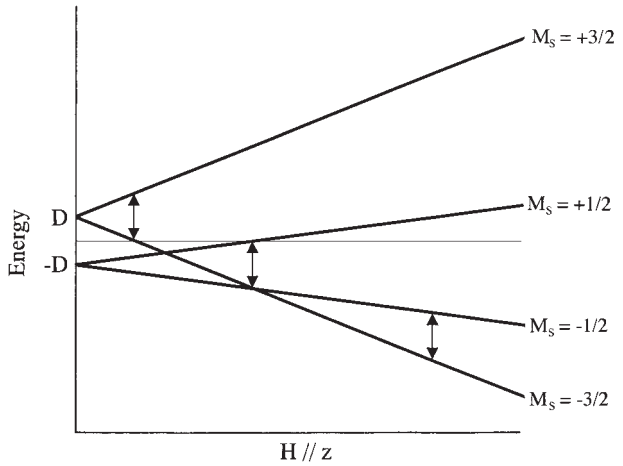

Fig. 6. Energy diagram of $S_T = 3/2$ under zero-field splitting and magnetic field.

Based on the isotropic Heisenberg model ($\boldsymbol{H} = -2\Sigma J_{ij}\boldsymbol{S}_i\boldsymbol{S}_j$) and using the energy diagram of Fig. 6, the magnetic susceptibility expression is derived as follows:

$$\chi_{\parallel} = \{Ng_z^2\beta^2/4k(T-\theta)\} \times \{1 + 9\exp(-2D/kT) + \exp[-(3J+D)/kT]\}/\{1 + \exp(-2D/kT) + \exp[-(3J+D)/kT]\} + N\alpha \quad (1)$$

In this expression, N is Avogadro's number, β is the Bohr magneton, k is the Boltzmann constant, T is the absolute temperature, J is the exchange integral, and $N\alpha$ is the temperature-independent paramagnetism. The Weiss constant θ is introduced as the correction term for contributions other than the zero-field splitting. In magnetic simulations using Eq. 1, the D and g values obtained by the above EPR analysis are used. As indicated by the solid curve in Fig. 5, the cryomagnetic property of **1** is well reproduced with this equation using $J = +22.0$ cm^{-1}, $\theta = -0.50$ K and $N\alpha = 300 \times 10^{-6}$ cm^3 mol^{-1}. The discrepancy factor defined as $R(\chi) = [\Sigma(\chi_{obsd} - \chi_{calcd})^2/\Sigma(\chi_{obsd})^2]^{1/2}$ was 4.67×10^{-2}. The energy separation between the $S_T = 3/2$ ground state and the $S_T = 1/2$ excited state is 66 cm^{-1} ($= 3J$).

The magnetic exchange integral $J_{MM'}$ in a dinuclear MM′ complex is expressed by the mean of the individual magnetic interactions:[22]

$$J_{MM'} = \Sigma j(k,l)/n_M n_{M'} \quad (2)$$

where n_M and $n_{M'}$ denote the number of unpaired electrons on M and M′, respectively, and $j(k,l)$ is the exchange integral between the unpaired electron on the k orbital of M and the unpaired electron on the l orbital of M′. In the present case, Co^{II} has one unpaired electron on its d_{z^2} orbital and Ni^{II} has two unpaired electrons on its d_{z^2} and $d_{x^2-y^2}$ orbitals. The exchange integral of **1** is expressed as $J_{CoNi} = [j(z^2, x^2-y^2) + j(z^2, z^2)]/2$. The $j(z^2, x^2-y^2)$ term must be positive due to the orthogonality of the magnetic orbitals, d_{z^2}(Co) $\perp$ $d_{x^2-y^2}$(Ni). The $j(z^2, z^2)$ term can be negative but must be small because the d_{z^2}-based magnetic orbitals, d_{z^2}(Co) and d_{z^2}(Ni), are only weakly delocalized toward the bridging phenolic oxygen atoms.[23] Thus, $j(z^2, x^2-y^2)$ is the dominant

term determining the positive overall exchange integral ($J = +22$ cm^{-1}) in **1**.

Conclusion

The heterodinuclear complexes, $[CoM(L^{2,3})](ClO_4)_2 \cdot H_2O \cdot 0.5CH_3CN$ (M = Ni(**1**), Zn(**2**)), have been prepared and their physicochemical properties were examined. Complex **1** has a low-spin Co^{II} ($S = 1/2$) and a high-spin Ni^{II} ($S = 1$) and shows a ferromagnetic interaction between the two metal ions to afford $S_T = 3/2$ ground state. EPR signals observed for **1** in a frozen DMF solution at liquid nitrogen temperature are ascribed to the $S_T = 3/2$ ground state, exhibiting a zero-field splitting of $D = 0.095$ cm^{-1}. Magnetic simulation based on isotropic Heisenberg model and taking into consideration the zero-field splitting gave a positive exchange integral of $J = +22$ cm^{-1} for **1**. The ferromagnetic interaction is interpreted by the strict orthogonality of the magnetic orbitals, d_{z^2}(Co) $\perp$ $d_{x^2-y^2}$(Ni).

This work was supported by a Grant-in-Aid for Scientific Research Program (No. 14340208) from the Ministry of Education, Culture, Sports, Science and Technology. One of the authors (M. Ohba) thanks Precursory Research for Embryonic Science and Technology (PRESTO), JST for financial support.

References

1 O. Kahn, *Struct. Bonding (Berlin)*, **68**, 91 (1987).

2 S. J. Gruber, C. M. Harris, and E. Sinn, *J. Inorg. Nucl. Chem.*, **30**, 1805 (1968).

3 a) H. Ōkawa, Y. Nishida, M. Tanaka, and S. Kida, *Bull. Chem. Soc. Jpn.*, **50**, 127 (1977). b) N. Torihara, H. Ōkawa, and S. Kida, *Chem. Lett.*, **1978**, 1269.

4 a) O. Kahn, P. Tola, J. Galy, and H. Coudanne, *J. Am. Chem. Soc.*, **100**, 3931 (1978). b) O. Kahn, J. Galy, Y. Journaux, J. Jaud, and I. Morgenstern-Badarau, *J. Am. Chem. Soc.*, **104**, 2165 (1982).

5 S. L. Lambert, C. L. Spiro, R. F. Gagne, and D. N. Hendrickson, *Inorg. Chem.*, **21**, 68 (1982).

6 a) H. Ōkawa, J. Nishio, M. Ohba, M. Tadokoro, N. Matsumoto, M. Koikawa, S. Kida, and D. E. Fenton, *Inorg. Chem.*, **32**, 2949 (1993). b) S. Ohtsuka, M. Kodera, K. Motoda, M. Ohba, and H. Ōkawa, *J. Chem. Soc., Dalton Trans.*, **1995**, 2599. c) H. Wada, T. Aono, K. Motoda, M. Ohba, N. Matsumoto, and H. Ōkawa, *Inorg. Chim. Acta*, **246**, 13 (1996). d) T. Aono, H. Wada, M. Yonemura, H. Furutachi, M. Ohba, and H. Ōkawa, *J. Chem. Soc., Dalton Trans.*, **1977**, 3029. e) S. Kita, H. Furutachi, and H. Ōkawa, *Inorg. Chem.*, **38**, 4038 (1999).

7 a) M. Yonemura, Y. Matsumura, H. Furutachi, M. Ohba, H. Ōkawa, and D. E. Fenton, *Inorg. Chem.*, **36**, 2711 (1997). b) M. Yonemura, M. Ohba, K. Takahashi, H. Ōkawa, and D. E. Fenton, *Inorg. Chim. Acta*, **283**, 72 (1998). c) M. Yonemura, Y. Nakamura, N. Usuki, and H. Ōkawa, *Proc.-Indian Acad. Sci., Chem. Sci.*, **112**, 291 (2000). d) M. Yonemura, N. Usuki, Y. Nakamura, and H. Ōkawa, *J. Chem. Soc., Dalton Trans.*, **2000**, 3624. e) M. Yonemura, K. Arimura, K. Inoue, N. Usuki, M. Ohba, and H. Ōkawa, *Inorg. Chem.*, **41**, 582 (2002).

8 O. Kahn, R. Claude, and H. Coudanne, *J. Chem. Soc., Chem. Commun.*, **1978**, 1012.

9 Y. Nishida and S. Kida, *Coord. Chem. Rev.*, **27**, 275 (1979).

10 Landolt-Börnstein, Neue Series II/11, Springer-Verlag, Berlin (1981).

11 D. A. Denton and H. Suschitzky, *J. Chem. Soc.*, **1963**, 4741.

12 TEXSAN, Molecular Structure Corporation, Houston, TX, 1985 and 1992.

13 M. Tadokoro, H. Sakiyama, N. Matsumoto, M. Kodera, H. Ōkawa, and S. Kida, *J. Chem. Soc., Dalton Trans.*, **1992**, 313.

14 a) H. Nishikawa and S. Yamada, *Bull. Chem. Soc. Jpn.*, **37**, 8 (1964). b) S. Yamada, *Coord. Chem. Rev.*, **1**, 415 (1966).

15 E. Cesarotti, M. Gullotti, A. Pasini, and R. Ugo, *J. Chem. Soc., Dalton Trans.*, **1977**, 757.

16 Y. Aratake, H. Ōkawa, E. Asato, H. Sakiyama, M. Kodera, S. Kida, and M. Sakamoto, *J. Chem. Soc., Dalton Trans.*, **1990**, 2941.

17 K. Inoue, M. Ohba, and H. Ōkawa, *Bull. Chem. Soc. Jpn.*, **75**, 99 (2002).

18 M. E. Frago, J. M. James, and V. C. G. Trew, *J. Chem. Soc. A*, **1967**, 820.

19 G. A. Nelson, "Coordination Chemistry of Macrocyclic Compounds," Plenum, New York (1979).

20 M. Calligaris, G. Nardin, and L. Randaccio, *Coord. Chem. Rev.*, **7**, 385 (1972).

21 B. R. McGarvey, *Transition Met. Chem. (N.Y.)*, **3**, 89 (1966).

22 J. H. Van Vleck, "The Theory of Electric and Magnetic Susceptibilities," Oxford University Press, Oxford (1932).

23 C. J. Cairns and D. H. Busch, *Coord. Chem. Rev.*, **69**, 1 (1986).